Pharmacological Research 113 (2016) 395–408

Contents lists available at ScienceDirect

Pharmacological Research

journal homepage: www.elsevier.com/locate/yphrs

Invited Review

Ibrutinib inhibition of Bruton protein-tyrosine kinase (BTK) in the treatment of B cell neoplasms

Robert Roskoski Jr.

Blue Ridge Institute for Medical Research, 3754 Brevard Road, Suite 116, Box 19, Horse Shoe, NC 28742-8814, United States

ARTICLE INFO

Article history:
Received 11 September 2016
Accepted 12 September 2016
Available online 15 September 2016

Chemical compounds studied in this article:
Bendamustine (PubMed CID: 65628)
Carfilzomib (PubMed CID: 11556711)
Dasatinib (PubMed CID: 3062316)
Fludarabine (PubMed CID: 657237)
Ibrutinib (PubMed CID: 24821094)
Idelalisib (PubMed CID: 11625818)
Palbociclib (PubMed CID: 5330286)
Pomalidomide (PubMed CID: 134780)
Venetoclax (PubMed CID: 49846579)
Vistusertib (PubMed CID: 44200550)

Keywords:
Catalytic spine
Chronic lymphocytic leukemia
K/E/D/D
Mantle cell lymphoma
Waldenström macroglobulinemia

ABSTRACT

The Bruton non-receptor protein-tyrosine kinase (BTK), a deficiency of which leads to X-linked agammaglobulinemia, plays a central role in B cell antigen receptor signaling. Owing to the exclusivity of this enzyme in B cells, the acronym could represent B cell tyrosine kinase. BTK is activated by the Lyn and SYK protein kinases following activation of the B cell receptor. BTK in turn catalyzes the phosphorylation and activation of phospholipase Cγ2 leading to the downstream activation of the Ras/RAF/MEK/ERK pathway and the NF-κB pathways. Both pathways participate in the maturation of antibody-producing B cells. The BTK domains include a PH (pleckstrin homology) domain that interacts with membrane-associated phosphatidyl inositol trisphosphate, a TH (TEC homology) domain, which is followed by an SH3, SH2, and finally a protein kinase domain. Dysregulation of B cell receptor signaling occurs in several B cell neoplasms including mantle cell lymphoma, chronic lymphocytic leukemia, and Waldenström macroglobulinemia. Ibrutinib is FDA-approved as first-line or second line treatment for these diseases. The drug binds tightly in the ATP-binding pocket of BTK making salt bridges with residues within the hinge that connects the two lobes of the enzyme; then its unsaturated acrylamide group forms a covalent bond with BTK cysteine 481 to form an inactive adduct. In addition to the treatment of various B cell lymphomas, ibrutinib is under clinical trials for the treatment of numerous solid tumors owing to the role of tumor-promoting inflammation in the pathogenesis of neoplastic diseases.

Contents

Abbreviations: AS, activation segment; CLL, chronic lymphocytic leukemia; CS or C-spine, catalytic spine; CL, catalytic loop; HΦ or Φ, hydrophobic; IP_3, inositol 1,4,5 trisphosphate; IP_6, inositol 1,2,3,4,5,6 hexakisphosphate; MCL, mantle cell lymphoma; MW, molecular weight; NSCLC, non-small cell lung cancer; PKA, protein kinase A; PIP_2, phosphatidyl inositol 4,5 bisphosphate; PIP_3, phosphatidyl inositol 3,4,5 trisphosphate; RA, rheumatoid arthritis; RS or R-spine, regulatory spine; Sh1, shell residue 1; WM, Waldenström macroglobulinemia.

E-mail address: rrj@brimr.org

http://dx.doi.org/10.1016/j.phrs.2016.09.011
1043-6618/

1. The role of Bruton protein-tyrosine kinase in B cell antigen receptor signaling

The Bruton kinase was originally identified in 1993 as a non-receptor protein-tyrosine kinase that is defective in X-linked agammaglobulinemia [1–4]. B lymphocytes and immunoglobulins are almost completely nonexistent in affected males with this rare affliction making them susceptible to infections, but they respond favorably to parenteral injections of human immunoglobulins [5]. Patients with this disorder have no significant alterations in cells other than B cells, and this observation is consonant with the restriction of clinical features to B cell immunity. Moreover, the X-linked immunodeficiency (XID) phenotype in the CBA/N strain of mice results from an R28C mutation near the amino-terminus of BTK, which is outside of the enzyme protein kinase domain [4].

During development, each B cell recombines immunoglobulin variable (V), diversity (D), and junction genes (J) thereby forming a unique sequence that establishes the antigen-binding site of the B cell receptor [6]. B cell receptor signaling requires a network of protein kinases and adaptors that mediate antigen stimulation to intracellular responses. The B cell receptor complex consists of the receptor bound to a disulfide-linked Igα-Igβ heterodimer. After antigen stimulation of the receptor, the Src family kinase Lyn catalyzes the phosphorylation of pairs of tyrosine residues in Igα-Igβ immunoreceptor tyrosine-based activation motifs (ITAMs) thus creating a docking site for the two SH2 domains of SYK (spleen tyrosine kinase) [7]. SYK attracts and activates PI3 kinase-δ, which catalyzes the conversion of membrane-associated phosphatidyl inositol 4,5 bis-phosphate (PIP_2) to phosphatidyl inositol 3,4,5-trisphosphate (PIP_3). The amino-terminal PH lipid-interaction module of BTK is attracted to PIP_3 thereby allowing SYK and Lyn to catalyze the *trans*-phosphorylation of BTK at Tyr551 within the activation segment that results in enzyme activation. The attraction of BTK dimers to PIP_3 molecules within the membrane can also result in activation segment *trans*-autophosphorylation and activation.

BTK catalyzes the phosphorylation of PLCγ2 at residues Tyr753 and Tyr759 resulting in an increase in phospholipase activity [8]. PLCγ2 catalyzes the hydrolysis of PIP_2 to generate inositol trisphosphate (IP_3) and diacylglycerol (DAG). IP_3 releases Ca^{2+} from intracellular stores, which activates PLCγ2. In turn, DAG and Ca^{2+} activate PKCβ, which leads to the activation of the Ras/RAF/MEK/ERK signaling module that promotes cell growth and proliferation [9–12]. PKCβ also activates the NF-κB pathway by means of a scaffold complex that includes CARD11 (caspase recruitment domain-containing protein 11), BCL10 (B cell lymphoma protein 10), and MALT1 (mucosa-associated lymphoid tissue lymphoma translocation protein 1) (Fig. 1). IκBα (inhibitor of kappa B-α) inactivates the NF-κB transcription factor by masking the nuclear localization signals of NF-κB and keeps it sequestered in an inactive state in the cytoplasm. The inhibitor of κB kinase (IKK) catalyzes the phosphorylation of the inhibitory IκBα, which results in its (i) dissociation from NF-κB, (ii) ubiquitylation, and (iii) proteosomal degradation. The unsequestered NF-κB translocates into the nucleus and activates the expression of more than 150 genes. NF-κB is a rapidly acting transcription factor that regulates, *inter alia*, cell survival and cytokine production. Additionally, BTK plays an essential role in the chemokine-mediated homing and adhesion of B cells [13]. As a result of BTK inhibition, B cells may be released from lymphatic tissue into the blood stream, which is commonly observed after treatment with ibrutinib. Besides its role in B cell antigen receptor signaling, BTK also participates in chemokine and Toll-like receptor signal transduction [8].

In contrast to the oncogenic activating *B-RAF V600E* mutation in melanoma and the *JAK2 V617F* mutation in polycythemia vera as well as numerous activating *EGFR/ERBB1* mutations in lung cancer, no activating mutations in BTK have been described in B cell neoplasms [8,9,12]. However, it appears that there is a chronic increase in B cell antigen receptor signaling in various B cell lymphomas [8]. Many lymphomas maintain B cell receptor signaling by responding to foreign or self antigens within the tumor microenvironment; the preponderance of evidence favors the interaction with self antigens. B cell proliferation that is driven by such antigens is essential for the pathogenesis of these afflictions. Moreover, sustained activity of the B cell receptor pathway is required for lymphocyte survival.

2. Biochemistry of the Bruton protein-tyrosine kinase

2.1. Architecture of BTK

BTK belongs to the TEC family of non-receptor protein-tyrosine kinases including BTK, TEC, ITK (inducible T cell kinase), TXK (also known as RLK, resting lymphocyte kinase), and BMX (bone marrow-expressed kinase) [14]. BTK contains a short amino-terminal pleckstrin homology (PH) domain, a TEC homology (TH) domain, followed by an SH3, SH2, and carboxyterminal protein kinase domain (Fig. 2A), which is an architecture shared with the other members of TEC family of protein kinases. This architecture is similar to that of the Src family of protein kinases except that they lack the PH and TH domains, but they contain a myristoylated amino-terminal domain, which is responsible for their binding to the plasma membrane (Fig. 2B) [15,16]. In contrast, the PH domain of the TEC family is attracted to membrane-associated PIP_3, which is responsible for their membrane-localization. Src possesses a carboxyterminal tail inhibitory protein-tyrosine phosphorylation site that binds intramolecularly with its SH2 domain to form an autoinhibited enzyme. BTK lacks this phosphorylation site indicating that the mechanism for the interconversion of active and inactive forms of BTK differs in detail from that of Src as described in Section 2.5.

BTK catalyzes the phosphorylation of protein-tyrosine residues in substrates such as PLCγ2. Members of the PLCγ2 family possess an intricate architecture consisting of an N-terminal pleckstrin homology domain, four EF hands, an X domain, a second PH domain containing two SH2 and one SH3 domain followed by a Y domain, a C2 domain, and C-terminal domain; the catalytic residues reside in the split X and Y segments [17]. The PLCγ2 phosphorylation sites (Y753, Y759) encompass the sequence ^{751}SLYDVSRMYV^{760}. These residues occur between the second PLCγ2 SH2 domain and the following SH3 domain. The stoichiometry of the protein kinase reaction is given by the following chemical equation:

$$MgATP^{1-} + \text{protein–O : H} \rightarrow \text{protein–O : } PO_3{}^{2-} + MgADP + H^+$$

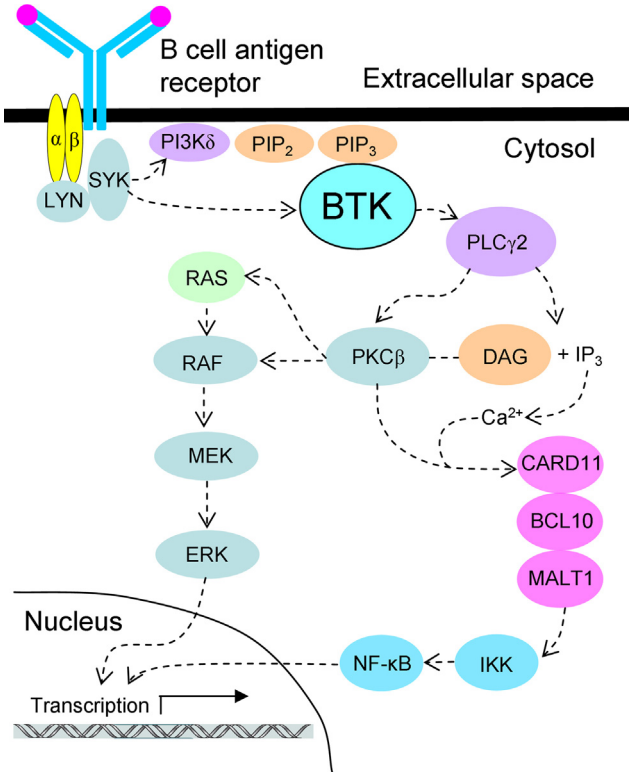

Fig. 1. Role of the Bruton protein-tyrosine kinase in B cell receptor signaling. The dashed arrows indicate that several steps may be involved.

Note that the phosphorylium ion (PO_3^{2-}) is transferred from ATP to the protein substrate and not the phosphate (OPO_3^{2-}) group.

2.2. Primary structure of BTK

Hanks and Hunter analyzed the sequences of about 60 protein kinases from various families and divided the primary structures into 12 domains (I-VIA,VIB-XI) [18]. The catalytic domains of protein kinases contain ≈250–300 amino acid residues. Domain I of BTK is called the glycine-rich loop (GRL) and contains a GxGxΦG signature (^{409}GTGQFG^{414}), where Φ refers to a hydrophobic residue, and in the case of BTK the hydrophobic residue is phenylalanine. The glycine-rich loop occurs between the β1- and β2-strands and overlays the ATP-binding site (Fig. 3A). Owing to its role in ATP binding and ADP release, the glycine-rich loop must be flexible. Domain II of BTK contains a conserved Ala-Xxx-Lys (^{428}AIK^{430}) sequence in the β3-strand and domain III contains a conserved glutamate (E445) in the αC-helix that forms an ionic bond with the conserved lysine in the active protein kinase conformation. Domain VIB of BTK contains a conserved HRD sequence, which forms part of the catalytic loop (^{519}HRDLAARN^{526}). Domain VII contains a ^{539}DFG^{541} signature and domain VIII contains a ^{565}PPE^{568} sequence, which together represent the beginning and end of the protein kinase activation segment; however, the end of the activation segment of most protein kinases consists of an APE signature. The remaining domains make up the αF–αI helices. The X-ray structure of PKA provided an invaluable framework for comprehending the role of the 12 domains on the protein kinase mechanism, as described next.

2.3. The secondary and tertiary structure of BTK and the K/E/D/D motif

The determination of the X-ray crystal structure of the catalytic subunit of PKA bound to a polypeptide protein kinase antagonist by Susan Taylor's group has enlightened our views on the fundamental biochemistry of the entire protein kinase enzyme family (PDB ID: 2CPK) [19,20]. All protein kinases including the Bruton protein-tyrosine kinase have a small amino-terminal lobe and large carboxyterminal lobe [21]. The amino-terminal lobe contains five conserved β-strands (β1–5) and a regulatory αC-helix and the large lobe contains four short strands (β6–β9) and seven conserved helices (αD–αI and αEF). A cleft between the small and large lobes serves as a binding site for ATP. Of the hundreds of protein kinase domain structures that have been reported, all of them have this fundamental protein kinase fold first described for PKA [19,20].

Essentially all functional protein kinases contain a K/E/D/D (Lys/Glu/Asp/Asp) signature that plays crucial mechanistic roles in the protein kinase reaction (Table 1) [12]. The lysine and glutamate occur within the small lobe and the two aspartate residues occur within the large lobe. Although both lobes contribute to ATP binding, the amino-terminal lobe plays a key role in this process. K430 (the K of K/E/D/D) of the β3-strand of BTK holds the α- and β-phosphates in position (Fig. 3A). The carboxylate group of E445 (the E of K/E/D/D) of the αC-helix forms an ionic bond with the ε-amino group of K430 and serves to stabilize its interactions with these phosphates. The presence of an ionic bond between the β3-lysine and the αC-glutamate is required for the formation of active protein

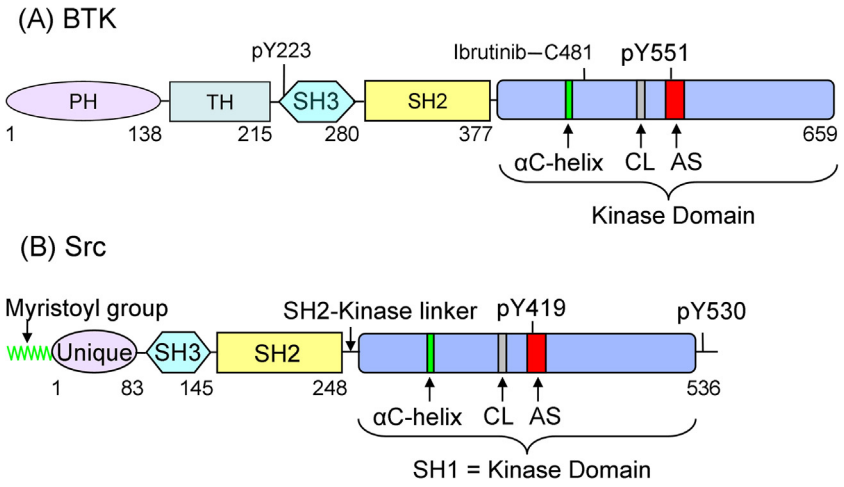

Fig. 2. Comparison of the architecture of (A) Bruton protein-tyrosine kinase and (B) Src. The relative size of each domain is indicated by the amino acid residue number given below. Ibrutinib binds covalently with C481. AS, activation segment; CL, catalytic loop; PH, pleckstrin homology domain; pY, phosphotyrosine; TH, TEC homology domain.

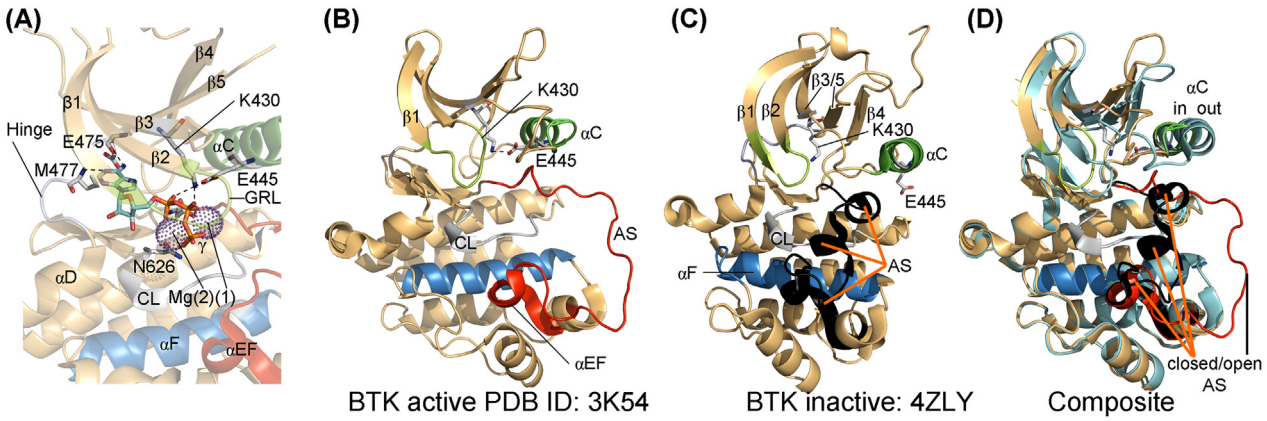

Fig. 3. (A) ATP-binding site of active BTK. (B) Overall structure of the active BTK protein-kinase domain. (C) Overall structure of the inactive BTK protein-kinase domain. (D) Superposition of the active and inactive BTK protein-kinase domains. AS, activation segment; CL, catalytic loop; GRL, Gly-rich loop. Figs. 3, 4, 5B/C/D and Fig. 6C/D were prepared using the PyMOL Molecular Graphics System Version 1.5.0.4 Schrödinger, LLC.

Table 1
Important residues in human BTK.[a]

		Inferred function	Hanks no.[b]
N-lobe			
Glycine-rich loop: GxGxΦG	^{409}GTGQFG^{414}	Anchors ATP β-phosphate	I
β3-K (K of K/E/D/D)	K430	Forms salt bridges with ATP α- and β-phosphates	II
αC-E (E of K/E/D/D)	E445	Forms ion pair with β3-K	III
Hinge residues	^{475}EYMANG^{480}	Connects N- and C-lobes	V
C-lobe			
αE-AS loop and AS HΦ-interaction	F517-V546	Stabilizes AS	VIb-VII
Catalytic loop HRD (first D of K/E/D/D)	D521	Catalytic base (abstracts proton)	VIb
Catalytic loop Asn (N)	N526	Chelates Mg^{2+}(2)	VIb
Activation segment	539–567	Positions protein substrate	VII-VIII
AS DFG (second D of K/E/D/D)	D539	Chelates Mg^{2+}(1)	VII
AS phosphorylation site	Y551	Stabilizes the AS after phosphorylation	VIII
PPE, end of AS	565–567	Interacts with the αHI loop and stabilizes the AS	VIII
UniProt KB ID	Q06187		

[a] AS, activation segment.
[b] From Ref. [18].

kinase conformation, which corresponds to an "αC-in" structure (Fig. 3B). In contrast K430 and E445 of the inactive enzyme fail to make contact, which corresponds to an "αC-out" structure (Fig. 3C). The αC-in conformation is necessary, but not sufficient, for the expression of catalytic activity.

The carboxyterminal lobe makes a major contribution to protein/peptide substrate binding and participates in the catalytic cycle. Two Mg^{2+} ions participate in a single catalytic cycle of several protein kinases [16] and are most likely required for the functioning of BTK. By inference, D539 (the DFG-D and the first D of K/E/D/D) binds to Mg^{2+}(1), which in turn binds to the β- and γ-phosphates of ATP. In this active conformation, the DFG-D is directed inward toward the active site. In the inactive form of many protein kinases, the DFG-D points outward from the active site. BTK N526 of the catalytic loop binds Mg^{2+}(2), which in turn binds to the α- and γ-phosphates of ATP. The activation segment of the BTK active state forms an open structure that allows protein/peptide binding (Fig. 3B). The activation segment in the dormant enzyme forms a closed, compact structure that blocks protein/peptide binding (Fig. 3C). Fig. 3D is a composite that illustrates the differences in the conformations of the αC-helix (in/active, out/inactive) and activation segment (open/active, closed/inactive). The active and inactive BTK contain an additional helix (αEF) near the end of the activation segment, which occurs in most protein kinases. The exocyclic 6-amino nitrogen of ATP characteristically forms a hydrogen bond with the carbonyl backbone residue of the first BTK hinge residue (E475) that connects the small and large lobes of the protein kinase domain and the *N*1 nitrogen of the adenine base forms a second hydrogen bond with the N—H group of the third hinge residue (M477). As discussed later, most small-molecule steady-state ATP competitive inhibitors of BTK and other protein kinases make hydrogen bonds with the backbone residues of the connecting hinge.

The activation segment is responsible for both protein-substrate binding and catalytic efficiency [22]. This segment in BTK contains a phosphorylatable tyrosine. The segment is spatially located near the amino-terminus of the αC-helix and the conserved HRD segment of the catalytic loop. The interaction of these entities is hydrophobic in nature. As is the case for most protein kinases [23], phosphorylation of a residue within the activation segment (tyrosine for the BTK) converts an inactive enzyme to an active one [24]. The activation segment of BTK and other protein kinases is further stabilized by hydrophobic interactions between an amino acid two residues N-terminal to the HRD-H of the catalytic loop (F517) and seven residues C-terminal to the DFG-D (V546) within the activation segment.

The catalytic loop surrounding the actual site of phosphoryl transfer within the large lobe consists of HRDLAARN in BTK. The catalytic aspartate (D521) in BTK, which is the first D of K/E/D/D serves as a base that accepts a proton from the tyrosyl —OH group (Fig. 4). The AAR sequence in the catalytic loop occurs in many receptor protein-tyrosine kinases such as EGFR and PDGFR and RAA occurs in many non-receptor protein-tyrosine kinases such as Src

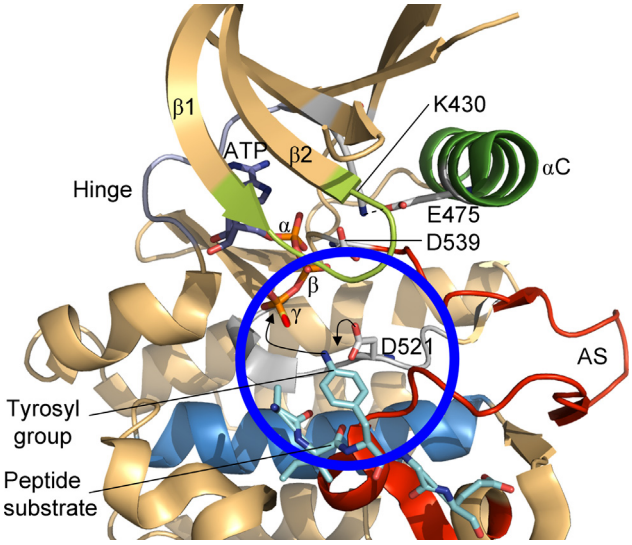

Fig. 4. Mechanism of the BTK catalyzed reaction. The chemistry occurs within the blue circle.

Table 2
Spine and shell residues of murine PKA and human BTK.

	Symbol	PKA[a]	BTK
Regulatory spine			
β4-strand (N-lobe)	RS4	L106	L460
C-helix (N-lobe)	RS3	L95	M449
Activation loop F of DFG (C-lobe)	RS2	F185	F540
Catalytic loop Y/H (C-lobe)	RS1	Y164	H519
F-helix (C-lobe)	RS0	D220	D579
R-shell			
Two residues upstream from the gatekeeper	Sh3	M118	I472
Gatekeeper, end of β5-strand	Sh2	M120	T474
αC-β4 loop	Sh1	V104	V458
Catalytic spine			
β2-strand (N-lobe)	CS8	V57	V416
β3-AxK motif (N-lobe)	CS7	A70	A428
β7-strand (C-lobe)	CS6	L173	L528
β7-strand (C-lobe)	CS5	I174	V529
β7-strand (C-lobe)	CS4	L172	C527
D-helix (C-lobe)	CS3	M128	L482
F-helix (C-lobe)	CS2	L227	L586
F-helix (C-lobe)	CS1	M231	I590

[a] From Refs. [25,26,29].

[18]. Thus, the occurrence of AAR in the BTK non-receptor protein kinase is somewhat anomalous.

2.4. Active and inactive BTK hydrophobic spines

Kornev et al. examined the structures of the active and inactive conformations of about two dozen protein kinases and they established the role of crucial residues by a local spatial pattern alignment algorithm [25,26]. Their investigation led to a taxonomy of eight hydrophobic residues as a catalytic or C-spine and four hydrophobic residues that make up a regulatory or R-spine. Each spine consists of amino acids occurring in both the small and large lobes. The R-spine contains a residue from the αC-helix and from the activation loop, both of which are key components in determining active and inactive states. The adenine base of ATP represents a part of the catalytic spine. The R-spine properly positions the peptide/protein substrate and the C-spine positions ATP within the active site thus enabling catalytic activity. Moreover, the proper arrangement of both spines is required for the creation of an active protein kinase as described for the Janus kinases, cyclin-dependent protein kinases, Src, EGFR, ERK1/2, and MEK1/2 [10,11,16,27,28].

The prototypical protein kinase regulatory spine consists of the HRD-His of the catalytic loop, the DFG-Phe of the activation segment, a residue near the carboxyterminal end of the αC-helix (four residues C-terminal to the conserved αC-glutamate), and a residue near the beginning of the β4-strand [25,26]. The backbone of the HRD-His is anchored to the internal hydrophobic αF-helix by a hydrogen bond to an invariant aspartate residue. Going from the bottom to the top of the spine, Meharena et al. labeled the R-spine residues RS0–RS4 (Fig. 5A and B) [29]. The R-spine of active BTK is nearly linear while that of the dormant enzyme is broken with RS3 displaced (Fig. 5B and C).

The protein kinase catalytic spine is made up of residues from both the small and large lobes and it is completed by the adenine portion of ATP (Fig. 5A) [26,29]. The two residues of the small lobe of protein kinase domains that interact with the adenine component of ATP include an invariant valine residue at the beginning of the β2-strand (CS7) and an invariant alanine from the conserved AxK of the β3-strand (CS8). Furthermore, a hydrophobic residue from the β7-strand (CS6) interacts with the adenine base. This CS6 residue is flanked by two hydrophobic residues labeled CS4 and CS5 that make hydrophobic contact with the CS3 residue near the beginning of the αD-helix. These three residues (CS4/5/6) immediately follow the asparagine residue of the catalytic loop (HRDxxxxN). Finally, CS3 and CS4 make contact with the CS1 and CS2 residues of the αF-helix to form a complete catalytic spine (Fig. 5A and B) [30]. Importantly, the hydrophobic αF-helix anchors both the catalytic and regulatory spines. Furthermore, both spines play an important role in placing the protein kinase catalytic residues in an active conformation. When comparing the locations of the spinal residues, the greatest divergence in the structures between the active and inactive BTK domains involve RS3 (Fig. 5D).

Using site-directed mutagenesis methodology, Meharena et al. identified three residues in protein kinase A that stabilize the R-spine, which they labeled Sh1–Sh3, where Sh refers to shell [29]. The Sh2 residue corresponds to the gatekeeper residue. The gatekeeper label indicates the role that this amino acid plays in controlling access to a back cleft [31], which is sometimes called the back pocket or hydrophobic pocket II (HPII). The amino acids that make up the spines were identified by their locations in active and inactive proteins based upon their three-dimensional X-ray crystallographic structures [25,26]. This contrasts with the identification of the APE, DFG, or HRD signatures, which is based upon their primary structures [18]. Table 2 provides a summary of the spine and shell residues of the Bruton tyrosine kinase. Of importance in determining drug specificity, small molecule protein kinase therapeutic antagonists generally interact with residues that make up the C-spine and sometimes the R-spine and shell residues [30].

2.5. Interconversion of inactive and active BTK

Wang et al. performed biochemical and structural studies on BTK that revealed the molecular mechanism of its autoinhibition and activation [32]. Although the overall modular structure of BTK and Src are similar (Fig. 2), the former contains an amino-terminal PH-TH domain, but it lacks an inhibitory C-terminal phosphorylation site. Despite these differences, autoinhibited BTK adopts a compact conformation that resembles that of the Src family kinases. The PH-TH module binds PIP_3 at a canonical binding site and IP_6 (inositol 1–6-hexakisphosphate) at a newly discovered peripheral binding site. This module acts in conjunction with the SH2 and SH3 domains to stabilize the inactive conformation (Fig. 6). The PH-TH domain binds in a groove between the kinase linker and the αC-helix. This interaction helps to stabilize the inactive conformation and blocks a shift in the αC-helix that is required to form the active

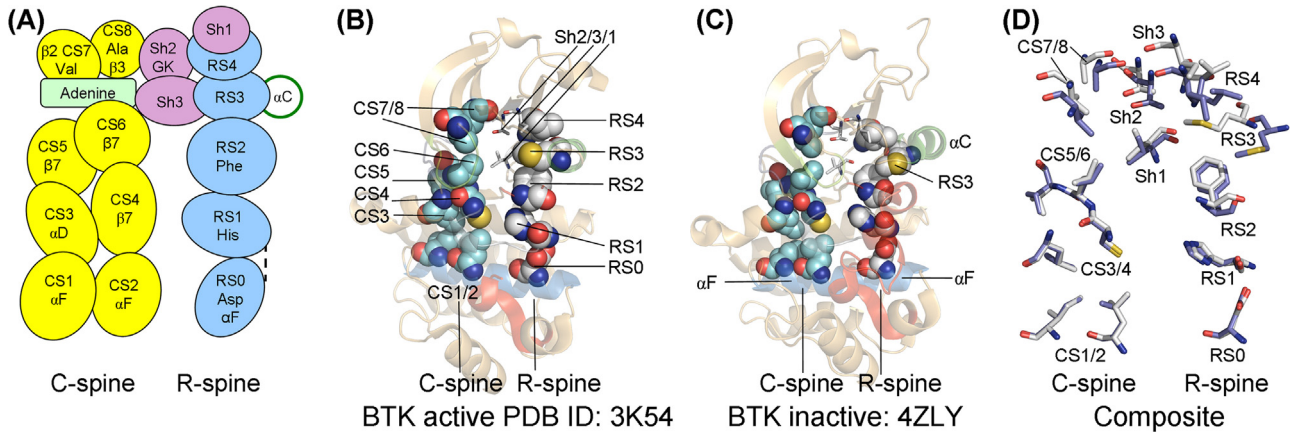

Fig. 5. The catalytic and regulatory spines and shell residues of BTK. (A) Spine labels. (B) The catalytic and regulatory spines of an active BTK. (C) The spines of an inactive BTK illustrating the displacement of RS3 as observed with the αC out conformation. (D) Superposition of active and inactive catalytic and regulatory spines and shell residues. Most residues are superimposable except for RS3, CS7/8, Sh2, and Sh3. Residues from the active enzyme are colored gray and those from the inactive enzyme are colored blue.

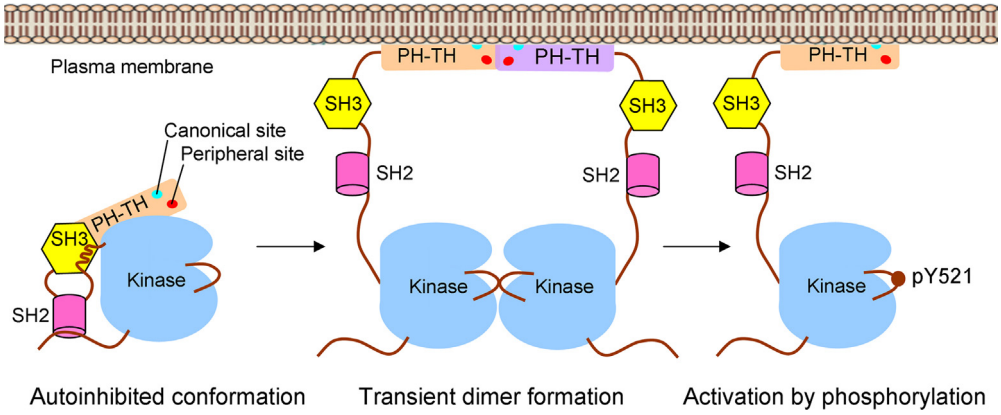

Fig. 6. Conversion of inactive to active BTK following recruitment by PIP_3 to the plasma membrane. PH-TH, pleckstrin homology-TEC homology domain. Adapted from Ref. [32].

conformation. The SH3 domain interacts with a polyproline type-II helix present within the SH2-kinase linker, which in turn interacts with and stabilizes the N-lobe of the protein kinase domain. The SH2 domain interacts with both the C-lobe and C-terminal tail while the PH-TH domain interacts with and immobilizes the N-lobe.

Following B cell receptor activation of PI3K and the generation of PIP_3, the canonical PIP_3-binding site in the PH-TH module is attracted to the plasma membrane by a process that disrupts the compact inactive conformation [32]. The association of two enzyme molecules leads to the *trans*-phosphorylation of Tyr521 within the activation segment of one or both proteins thereby leading to the activated state. The phosphorylation of Tyr223 within the SH3 domain also occurs; this modification does not alter the catalytic activity of BTK, but it may change the selectivity toward its binding partners. Activated BTK can then participate in the signal transduction module depicted in Fig. 1. These investigators also found that the hydrophilic IP_6 binds to a peripheral binding site and induces BTK dimer formation in a membrane-independent process resulting in ATP-dependent *trans*-phosphorylation of the activation segment and enzyme activation. The pathway for the conversion of the active phosphorylated BTK to the inactive conformation has not been deciphered. However, it must involve dephosphorylation of pY521 within the activation segment, detachment of the enzyme from membrane-associated PIP_3 followed by dephosphorylation of PIP_3, or dephosphorylation of IP_6 in the membrane-independent activation process.

3. FDA-approved ibrutinib disease targets

3.1. Mantle cell lymphoma (MCL)

People with mantle cell lymphoma, which makes up about 6% of non-Hodgkin lymphomas, usually present with palpable lymphadenopathy with a median age of about 65 years [33]. The male/female ratio is 4/1. Nearly 70% of patients will be at stage IV at the time of diagnosis with peripheral blood, bone marrow, spleen, and gastrointestinal tract involvement. The historical median overall survival in people with newly diagnosed MCL is three to four years. These B cell lymphomas have a t(11:14) (q13:q32) chromosomal translocation between the immunoglobulin heavy chain gene on chromosome 14 and the *CCND1* gene on chromosome 11, which leads to the constitutive overexpression of cyclin D1. Cyclin D1 activates CDK4 and CDK6 leading to G1-S cell cycle progression [28]. The fundamental unit of lymphatic tissues is the lymphatic nodule, which consists of a germinal center with an outer ring or mantle of small lymphocytes, which is the initial location of the cells of this lymphoma. Previous standard therapies for mantle cell lymphoma include (i) the rituximab-CHOP regimen of cyclophosphamide, hydroxydaunorubicin (doxorubicin), oncovin (vincristine), and prednisone combined with rituximab, (ii) cyclophosphamide, oncovin, hydroxydaunorubicin, dexamethasone, cytarabine, and methotrexate, (iii) bortezomib, or (iv)

Table 3
Drugs used in the treatment of various malignancies.

Drug	Disease targets	FDA-approved targets	Mechanism
Small molecule agents			
Acalabrutinib	CLL	None	An orally effective irreversible BTK inhibitor
Bortezomib	MCL, MM	MCL, MM	An injectable proteosome inhibitor
Buparlisib	Breast cancer, MCL	None	An orally effective pan-PI3 kinase inhibitor
Carfilzomib	MM	MM	An intravenous injectable proteosome inhibitor
CC-122	DLBCL	None	An orally effective immunomodulator that induces tumor cell apoptosis and inhibits angiogenesis
Dasatinib	ALL, CML	ALL, CML	An orally effective multi-protein kinase inhibitor with activity against BCR-Abl, BTK, Src, Lck, Yes, Fyn, Kit, EphA2, PDGFRβ
Dexamethasone	Inflammatory and neoplastic diseases	Inflammatory and neoplastic diseases	An orally effective glucocorticoid immunosuppressant
Everolimus	CRC, RCC, gastric or urothelial carcinomas	HER-2$^-$ breast cancer, RCC, PNET	An orally effective FKBP12/mTOR inhibitor
Ibrutinib	CLL, CLL with 17d deletion, MCL, WM	Same as disease targets	An orally effective irreversible BTK inhibitor
Idelalisib	CLL, FL, SLL	Same as disease targets	An orally effective PI3 kinase-δ inhibitor
Lenalidomide	MM, HL, NHL, CLL	MM, myelodysplastic syndrome	Similar to CC-122
Pacritinib	Myelofibrosis, AML, CLL, NSCLC, CRC	None	An orally effective JAK2 inhibitor that is on hold in clinical trials
Palbociclib	MCL, breast cancer	ER$^+$-HER-2$^-$ breast cancer	An orally effective CDK4/6 inhibitor
Pomalidomide	MM	MM	Similar to CC-122
Prednisone	Inflammatory and neoplastic diseases	Inflammatory and neoplastic diseases	An orally effective glucocorticoid immunosuppressant; part of the CHOP regimen
Selinexor	CLL, NHL, thymoma, CRC	None	An orally effective nuclear export inhibitor that prevents tumor suppressor proteins from exiting the nucleus
Temsirolimus	MCL, RCC	RCC	An injectable MKBP12/mTOR inhibitor
TGR-1202	CLL, FL, DLBCL	None	An orally effective PI3 kinase-δ inhibitor
Venetoclax	CLL	CLL with 17p deletion	An orally effective small molecule inhibitor of Bcl-2 leading to apoptosis, a BH3-mimetic
Vistusertib	DLBCL, many malignancies	None	An orally effective mTOR inhibitor
Cytotoxic agents			
Bendamustine	CLL, lymphoma	CLL, indolent B cell NHL	An injectable alkylating agent related to nitrogen mustards
Carboplatin	DLBCL, many solid tumors	About one dozen solid tumors	An injectable platinum-based anti-neoplastic agent that produces DNA cross links and interferes with DNA repair.
Chlorambucil	CLL, lymphomas, HD	Same as disease targets	An orally effective nitrogen mustard alkylating agent.
Cyclophosphamide	Burkitt lymphoma, NHL, Ovary	Numerous lymphomas, leukemias, and solid tumors	Similar to bendamustine except it can be given orally; part of the CHOP and FC-R regimens
Cytarabine	AML and other malignancies	ALL, AML, lymphomas	An injectable inhibitor of DNA and RNA polymerases and DNA replication
Docetaxel	CRC, RCC, gastric or urothelial carcinomas	A half dozen solid tumors	An injectable antimitotic that binds to microtubules
Etoposide	DLBCL, other malignancies	Various sarcomas, carcinomas, lymphomas, and leukemias	An injectable DNA topoisomerase II inhibitor that causes DNA strand breakage
Gemcitabine	Pancreatic carcinoma	Several solid tumors	An injectable nucleoside analog in which the hydrogen atoms on the 2′ carbon of deoxycytidine are replaced by fluorine atoms leading to the inhibition of ribonucleotide reductase and DNA synthesis
Hydroxydaunorubicin, or doxorubicin	CLL	Various leukemias, HL, MM, various solid tumors	An injectable drug that intercalates with DNA and inhibits the progression of topoisomerase II thereby inhibiting DNA replication; part of the CHOP regimen
Fludarabine	CLL	CLL	An injectable purine analog that inhibits ribonucleotide reductase and DNA polymerase-α thereby inhibiting DNA synthesis; part of the FC-R regimen
Idarubicin	AML	AML	An injectable drug that intercalates with DNA and inhibits the progression of topoisomerase II thereby inhibiting DNA replication; related to hydroxydaunorubicin
Ifosfamide	DLBCL, other tumors	Germ cell testicular carcinoma	See bendamustine
Methotrexate	Numerous malignancies, psoriasis, and RA	Same as disease targets	An orally effective agent that inhibits dihydrofolate reductase thereby decreasing the synthesis of tetrahydrofolate, which is required for the synthesis of thymidine as well as purine and pyrimidine bases

Table 3 (*Continued*)

Drug	Disease targets	FDA-approved targets	Mechanism
Oncovin, or vincristine	ALL, AML, CLL, HD, neuroblastoma, SCLC	ALL, AML, HD, neuroblastoma, rhabdomyosarcoma, SCLC, Wilm tumor	An injectable drug that binds to microtubules blocking metaphase; part of the CHOP regimen
Paclitaxel	CRC, RCC, gastric or urothelial carcinomas	A half dozen solid tumors	An injectable antimitotic that binds to microtubules
Monoclonal antibodies (given parenterally)			
Alemtuzumab	CLL, MS	CLL, MS	A humanized monoclonal antibody directed against CD52, which occurs on mature lymphocytes
Atezolizumab	CLL, metastatic urothelial carcinoma	Metastatic urothelial carcinoma	A humanized monoclonal antibody directed against programmed cell death receptor-1 and an immune checkpoint inhibitor
BI 836826	CLL	None	A chimeric monoclonal antibody directed against CD-37, which is a leukocyte antigen
Cetuximab	CRC, RCC, gastric or urothelial carcinomas	CRC, NSCLC, HNSCC	A chimeric monoclonal antibody directed against EGFR
Durvalumab	CLL, NSCLC, urothelial bladder cancer	None	A fully human monoclonal antibody directed against programmed cell death receptor-1 and an immune checkpoint inhibitor
Monalizumab	CLL, other malignancies	None	A humanized monoclonal antibody directed against killer cell lectin like receptor C1 (KCRC1) found in natural killer cells that function as a checkpoint inhibitor
Obinutuzumab	CLL	CLL, FL	A humanized monoclonal antibody directed against CD-20, which is found primarily on the surface of B cells
Ofatumumab	CLL, DLBCL, FL, MCL, MS, RA, WM	CLL	A fully human monoclonal antibody directed against CD-20.
Pembrolizumab	CLL, Melanoma, NSCLC, HNSCC	Melanoma, NSCLC, HNSCC	A humanized monoclonal antibody and an immune checkpoint inhibitor
Rituximab	CLL, NHL	CLL, NHL, RA, Wegener granulomatosis	A chimeric monoclonal antibody directed against CD-20; part of the FC-R regimen
Ublituximab	CLL	None	A chimeric monoclonal antibody directed against CD-20

ALL, acute lymphocytic leukemia; AML, acute myelogenous leukemia; DLBCL, diffuse large B cell myeloma; CHOP; cyclophosphamide, hydroxydaunorubicin, oncovin (vincristine), prednisone; CLL, chronic lymphocytic leukemia; CRC, colorectal cancer; ER^+, estrogen receptor positive; FC-R, fludarabine, cyclophosphamide, rituximab; FL, follicular B cell non-Hodgkin lymphoma; HD, Hodgkin disease; $HER\text{-}2^-$, human estrogen receptor negative; HL, hairy cell leukemia; HNSCC, head and neck squamous cell carcinoma; LCL, large cell lymphoma; MCL, mantle cell lymphoma; MM, multiple myeloma; MS, multiple sclerosis; NHL, non-Hodgkin lymphoma; NSCLC, non-small cell lung cancer; PI, phosphatidyl inositol; PNET, pancreatic neuroendocrine tumor; RA, rheumatoid arthritis; RCC, renal cell carcinoma; SCLC, small cell lung cancer; SLL, small lymphocytic lymphoma; WM, Waldenström macroglobulinemia.

lenalidomide [34] (See Table 3 for the mechanism of action of these agents).

Wang et al. performed a phase II clinical trial in 111 patients with relapsed or refractory mantle cell lymphoma most of whom had received previous bortezomib therapy [35]. They used computed tomographic and PET scans to assess tumor burden. They found that 21% had a complete response to oral ibrutinib while an additional 47% had a partial response (68% total). These investigators estimated that the overall survival was 58% at 18 months. Such responses had only been observed in patients receiving intensive cytotoxic chemotherapy regimens. Wang et al. reported that 18% of the subjects developed anemia and 18% developed thrombocytopenia [35]. Non-hematologic adverse events included diarrhea (50%), fatigue (41%), nausea (31%), peripheral edema (28%), and dyspnea (27%). Ibrutinib treatment led to a substantial increase in mantle cell lymphoma cells in the blood after 10 days followed by a decrease to baseline after 28 days. This transient increase was due to the liberation of these cells from the affected lymphatic tissues. The authors concluded that ibrutinib monotherapy was less stressful and more effective than previous standard therapies. Based upon these studies, the FDA approved ibrutinib for the treatment of mantle cell lymphoma in November 2013 [36].

3.2. Chronic lymphocytic leukemia (CLL)

Chronic lymphocytic leukemia, which is a clonal B cell disorder, is the most common type of leukemia in the Western hemisphere accounting for about 40% of all adult leukemias [37]. The age-adjusted incidence rate is 4.5 per 100,000 inhabitants in the United States, which amount to about 15,000 new cases per year. The median age at diagnosis is about ≈70 years of age. The diagnosis of CLL is often incidental and based upon routine blood counts. In symptomatic patients, fatigue, fever, and infections may be the presenting features. Physical examination may reveal cervical, axillary, and inguinal lymphadenopathy along with splenomegaly and hepatomegaly. A small percentage of patients with CLL progress into an aggressive large cell lymphoma (LCL) by a transformation that is called Richter syndrome. Laboratory studies indicate that CLL and LCL cells share identical clonal origins.

CLL patients have elevated lymphocyte counts with more than 5000 non-proliferating clonal mature B cells/μL persisting for more than three months [37]. These cells with scant cytoplasm have dense chromatin and they lack nucleoli. Such cells express B cell markers including CD23, CD19, CD5 antigen and they weakly express CD20 and surface membrane immunoglobulin. Recombination of variable (V), diversity (D), and joining (J) genes occurs in the pregerminal phase of B cell development. Somatic mutations are introduced in the VDJ rearrangement in normal B cells. Approximately 50% of CLL cases have somatic mutations in the IgV gene (*IGHV-M*) and thus arise from postgerminal B cells while a subset of CLL has unmutated IgV (*IGHV-UM*) that arises from naïve B cells. *IGHV-M* CLLs respond poorly to surface membrane immunoglobulin stimulation and CLL patients with this mutation have a favorable outcome.

Patients at early stages of CLL can be followed without specific therapy with a median survival greater than 10 years [36]. Patients

who present with bone marrow failure would ordinarily have a median survival of only 1.5 years and thus require initial therapy. The following agents have been approved by the FDA for the treatment of CLL: chlorambucil (1957), cyclophosphamide (1959), fludarabine (1991), alemtuzumab (2007), bendamustine (2008), ofatumumab (2009), rituximab in combination with fludarabine and cyclophosphamide (2010), obinutuzumab in combination with chlorambucil (2013) [36], and idelalisib (2014) (www.brimr.org/PKI/PKIs.htm).

The following guidelines for assessing the response of patients with CLL were established in 2008 [38,39]. A patient achieves a complete response if the following criteria are met within two months following the completion of the treatment: blood lymphocytes levels <4000/μL, lack of lymphadenopathy, lack of splenomegaly and hepatomegaly, lack of constitutional symptoms such as fatigue and weight loss, and normalization of blood counts without the use of erythropoietin or any other growth factors. If all of these criteria are met, a bone marrow aspirate should be performed and analyzed to confirm that a complete response has occurred. A patient achieves a partial response if two of the following criteria are met within two months following the completion of treatment: a 50% reduction or more from the baseline of (i) blood lymphocyte levels, (ii) lymphadenopathy, (iii) hepatomegaly, or (iv) splenomegaly and normalization of either peripheral blood neutrophils (>1500/μL), platelets (>100,000/μL), or hemoglobin (>11.0 g/μL). Disease progression occurs if any one of the following takes place: a change of at least 50% from baseline in (i) cytopenias, (ii) hepatomegaly, (iii) lymphadenopathy, (iv) lymphocyte levels, (v) splenomegaly, or if any new lesions appear.

Byrd et al. performed a phase II clinical trial in 85 patients with high risk relapsed or refractory CLL [40]. The overall response rate to oral ibrutinib was 71% and an additional 15–20% had a partial response with lymphocytosis. The response was independent of clinical and genomic risk factors present before treatment, including advanced-stage disease, the number of previous therapies, and the 17p13.1 deletion. At 26 months, the estimated progression-free survival rate was 75% and the rate of overall survival was 83%. Ibrutinib caused a transient increase in blood lymphocyte levels, which was concurrent with a reduction in lymph-node size, spleen size, or both. Continued treatment with ibrutinib led to resolution of this asymptomatic lymphocytosis. They found that ibrutinib did not result in a higher incidence of grade 3 or higher infections during the extended therapy. Grade 3/4 hematological toxicities included neutropenia (13%), thrombocytopenia (11%), and anemia (10%). The most common adverse events included diarrhea, fatigue, and nausea. Patients lacking the IgV mutation (*IGHC-UM*) exhibited an earlier resolution of lymphocytosis and were more frequently classified as having a response than those patients with the mutation. The durable remissions exhibited in this study lead to the approval of ibrutinib monotherapy for the treatment of CLL [36].

Byrd et al. reported on the results of a three-year follow-up of treatment-naïve and previously treated patients with CLL and small cell lymphoma (SLL) receiving ibrutinib monotherapy [41]. The estimated progression-free survival in treatment naïve patients was 96% at 30 months while it was 69% for previously treated patients. Of the 25 patients whose illness progressed while on ibrutinib, nearly all of them (23) had cytogenetic alterations such as 14 del(17p), 10 del(11q), or both. Of these 25 patients, several (8) had the Richter transformation. The estimated 30-month overall survival for the previously untreated patients was 97% and that for the previously treated patients was 79%. The del(17p) patients have a 30-month estimated overall survival rate of 65% while that of the del(11q) patients was 85% compared with 90% in the absence of either aberration. Adverse events included hypertension, pneumonia, neutropenia, thrombocytopenia, atrial fibrillation, diarrhea, fatigue, and sepsis. Except for hypertension, the incidence of these effects decreased from year-to-year as the treatment period lengthened. These studies demonstrate that ibrutinib controls CLL disease manifestations and is well tolerated for extended periods.

Although there are numerous caveats, the studies of Byrd et al. suggest that ibrutinib monotherapy should be considered as a standard first-line therapy, especially in older patients with numerous co-morbidities [41]. Side effects such as diarrhea and ecchymoses (spontaneous subcutaneous bleeding) are mostly mild and generally self-limited. The standard first-line therapy for patients younger than 65 years and lacking co-morbidities is fludarabine, cyclophosphamide, and the CD20-specific monoclonal rituximab (the FC-R regimen). Patients with a 11q deletion, which is considered as an adverse prognostic indicator, and patients with *IGHV-M* respond very well to the FC-R regimen. In contrast, patients with *IGHV-UM* cells have shorter remissions than those with the mutated genes [40]. Patients with a 17p13.1 deletion of the tumor suppressor protein p53 had a poor response to the FC-R regimen. For this reason, ibrutinib is approved by the FDA for the first-line treatment of patients with CLL possessing this deletion.

The development of resistance is a major problem with nearly all cancer therapies and the treatment of CLL with ibrutinib is not an exception [42]. Woyach et al. performed whole-exome sequencing in six patients prior to ibrutinib treatment and after acquired resistance became apparent [42]. Five of the patients had C481S mutations in BTK, two had mutations in PLCγ2, and one of the six patients had mutations in both proteins. Owing to the conversion of a BTK active-site cysteine to serine, this mutant protein fails to undergo covalent modification by ibrutinib. Moreover, the mutant protein had a fifty-fold higher K_D for ibrutinib than the wild type enzyme (10.4 vs. 0.2 nM). As expected, ibrutinib was much less effective in blocking BTK autophosphorylation and downstream signaling (ERK phosphorylation) in human embryonic kidney (HEK 293T) cells transfected with the C481S mutant than with the wild type enzyme. They identified a PLCγ2 R665W mutation in one of the patients with mutant BTK. Moreover, they identified PLCγ2 R665W, L845F, and S707Y mutations in another patient with wild type BTK. The S707Y mutation occurs within the autoinhibitory SH2 domain of PLCγ2 and results in constitutive activation. They demonstrated that transfection of the R665W or the L845F mutant protein into HEK 293T cells led to increased IgM antibody-mediated calcium flux that was not blocked by ibrutinib. Furthermore, ibrutinib was less effective in blocking the phosphorylation of ERK and AKT in response to IgM-antibody stimulation in cells bearing either of these two mutations. Accordingly, these investigators concluded that these PLCγ2 gain-of-function mutations could be relevant in conferring ibrutinib resistance.

Maddocks et al. conducted a follow up study on CLL resistance mutations in 13 patients [43], six of whom were included in the previous study [42]. Altogether, nine of the patients had C481S BTK mutations, three had mutations in PLCγ2, and three of the 13 patients had mutations in both proteins [43]. In addition to the BTK C481S mutation observed in eight patients, one patient possessed a C481F mutation and another patient possessed three BTK mutations: C481S, T474I, and T474S where T474 is the gatekeeper residue that forms a hydrogen bond with ibrutinib as described in Section 5. They also reported that one patient possessed a D334H mutation in PLCγ2 along with three BTK mutations: C481Y, C481R, L528W, the latter of which corresponds to CS6.

Johnson et al. reported that the wild type and C481S mutant of BTK had similar activity while the k_{cat} of the C481R mutant was about 1/12th that of the other enzymes [44]. Thus, substitution of the large charged arginine residue in place of the smaller cysteine decreases enzyme activity. The catalytic activity of the T474I gatekeeper mutant had about 70% of the activity as the wild type enzyme. Although one generally considers the size of the gatekeeper in terms of allowing access to an adjacent hydrophobic

pocket as being the important factor, the gatekeeper is the Sh2 residue, and substituting a large hydrophobic residue in this position might actually result in an increase in catalytic activity. For example, Azam et al. reported that the substitution of isoleucine or methionine for the threonine gatekeeper in the Abl, EGFR, PDGFRα/β, and Src results in the enhancement of enzyme activity [45]. The gatekeeper residue occurs near the top of the hydrophobic R-spine (Fig. 5A and B) and these investigators suggested that enzyme activation is related to the ability of the hydrophobic gatekeeper to strengthen the R-spine and promote the formation of the active conformation of the protein kinase domain. As noted above and in contrast to Abl and Src, the substitution of an isoleucine for the threonine gatekeeper failed to increase BTK activity. The reason for this anomalous behavior is unclear.

Because ibrutinib therapy has been used for only a few years, it is too early to know whether these mutations represent the only mechanisms for resistance or whether additional possibilities such as the activation of by-pass pathways will emerge in the future. We have no information on mechanisms of primary or acquired (secondary) resistance in patients with mantle cell lymphoma or Waldenström macroglobulinemia.

Cheng et al. studied the effects of BTK antagonists on the C481S mutant enzyme [46]. They found that dasatinib, a BCR-Abl, Src, Lck, Yes, Fyn, Kit, EphA2, PDGFRβ multi-kinase antagonist, inhibited wild type and mutant BTK. Dasatinib had previously been reported to inhibit wild type BTK with an IC_{50} of 5 nM; this compares favorably with the IC_{50} obtained vs. Abl of 14 nM [47]. Dasatinib is FDA approved for the treatment of Philadelphia chromosome positive ALL and CML where its drug target is presumed to be BCR-Abl. Cheng et al. found that idelalisib, a PLCγ2 antagonist approved by the FDA for the treatment of relapsed CLL, SLL, and follicular lymphoma, also inhibited the growth of patient CLL cells expressing the *C481S* mutation at clinically achievable concentrations [46].

3.3. Waldenström macroglobulinemia (WM)

This disorder is a B cell neoplasm associated with the accumulation of clonal immunoglobulin M secreting lymphoplasmacytic cells [48]. The age-adjusted incidence rate is about 0.38 per 100,000 inhabitants in the United States, which amounts to about 1300 cases per year. The median age at diagnosis is about ≈70 years of age and the male/female ratio is about 1.5/1. The disorder is quite heterogeneous and can present with fatigue, fever, chills, recurrent sinus and bronchial infections, headaches, diarrhea, and gastrointestinal cramping. Hepatosplenomegaly and lymphadenopathy may also be present. Elevated IgM levels (>7 g/dL) are more than 25 times greater than the normal value. Such high levels lead to an increase in serum viscosity, which may manifest itself as headaches, blurry vision, episodes of mental confusion, or nose bleeds. The presence of IgM monoclonal protein associated with more than 10% of clonal lymphoplasmacytic cells in the bone marrow will confirm the diagnosis.

A *MYD88* (myeloid differentiation primary response gene 88) L265P mutation is present in more than 90% of patients [49]. This gene product is an adapter protein that mediates Toll-like receptor signaling and innate immune responses. This gain-of-function mutation participates in the activation of NF-κB by means of BTK (Fig. 1) and the interleukin-1 receptor-associated kinases (IRAK1 and IRAK4). As a consequence of the *MYD88* mutation, BTK is constitutively activated in WM cells. Mutations in the *CXCR4* chemokine receptor occur in about one-third of WM patients. These mutations are like those observed in patients with the WHIM syndrome (warts, hypogammaglobulinemia, infections, and myelokathexis, where the latter term refers to the retention – kethexis – of neutrophils in the bone marrow). Stimulation of the *CXCR4* receptor is associated with lymphocyte chemotaxis.

A variety of therapies are used in the treatment of Waldenström macroglobulinemia [50,51]. These include rituximab as a first-line or second-line treatment with an overall response rate of 52% (no complete responses). The combination of rituximab with other agents is more effective than rituximab monotherapy. For example, the rituximab/thalidomide combination as first- or second-line treatments was somewhat more effective with an overall response rate of 64% and a complete response rate of 4%. The FC-R (fludarabine, cycloheximide, rituximab) first- and second-line treatments had an overall response rate of 79% and complete response rate of 12% while the DRC (dexamethasone, rituximab, cyclophosphamide) first-line regimen had an overall response rate of 83% with a complete response rate of 7%. Moreover, the rituximab/cladribine combination as first- or second-line treatment had an overall response rate of 90% and a complete response rate of 24% while a rituximab/bendamustine combination for relapsed or refractory WM had an overall response rate of 90% and a complete response rate of 60%. The rituximab-CHOP (cyclophosphamide, doxorubicin, vincristine, prednisone) protocol as a first-line therapy had an overall response rate of 94% and a complete response rate of 9% and a rituximab/fludarabine combination as second-line treatment had an overall response rate of 95% with a 5% complete response rate. Combination therapies without rituximab were also effective. For example, the CaRD (carfilzomib, cyclophosphamide, dexamethasone) protocol had an overall response rate of 87% and a complete response rate of 3% and first-line bortezomib monotherapy had an overall response rate of 96% with a complete response rate of 13%.

Treon et al. reported on a prospective clinical study using ibrutinib monotherapy on 63 symptomatic patients with WM who had received at least one previous treatment [49]. They found that oral ibrutinib treatment decreased the median serum IgM levels from 3.52 to 0.88 g/dL while the median hemoglobin levels increased from 10.5 g to 13.8 g/dL. They also found that the bone marrow involvement decreased from 60% to 25%. The overall response rate was 91% and it was highest in patients with the $MYD88^{L265P}CXCR4^{WT}$ genotype (100% overall response rate) followed by patients with the $MYD88^{L265P}CXCR4^{WHIM}$ (88%) and $MYD88^{WT}CXCR4^{WT}$ genotypes (71%). The estimated two-year progression-free survival among all patients was 69% and overall survival was 95%. The treatment related toxicities of grade 2 or higher included neutropenia (22%) and thrombocytopenia (14%). As a result these studies, ibrutinib was approved by FDA for the treatment of WM (www.brimr.org/PKI/PKIs.htm). Because patients with inactivating BTK mutations in X-linked agammaglobulinemia have an increased incidence of infections [5], it is surprising that there were not more reported cases of serious infections in the ibrutinib clinical trials.

4. Selected ibrutinib clinical trials

Ibrutinib alone or in combination with other medicines is being evaluated in more than 150 clinical trials (www.clinicaltrials.gov). The goal of these trials is to increase therapeutic efficacy and to mitigate the development of primary and acquired drug resistance. The following combinations are being tested for the treatment of chronic lymphocytic leukemia: (i) ibrutinib, fludarabine, cyclophosphamide, and obinutuzumab; (ii) ibrutinib with the standard combination of fludarabine, cyclophosphamide, and rituximab (FC-R); (iii) ibrutinib and bendamustine; (iv) ibrutinib and pacritinib; (v) ibrutinib and selinexor (vi) ibrutinib and venetoclax; (vii) ibrutinib vs. rituximab; (viii) ibrutinib vs. acalabrutinib; (ix) ibrutinib, rituximab, and lenalidomide; (x) ibrutinib vs. durvalumab; (xi) ibrutinib vs. ofatumumab; (xii) ibrutinib and atezolizumab, or obinutuzumab, or monalizumab, or obinutuzumab,

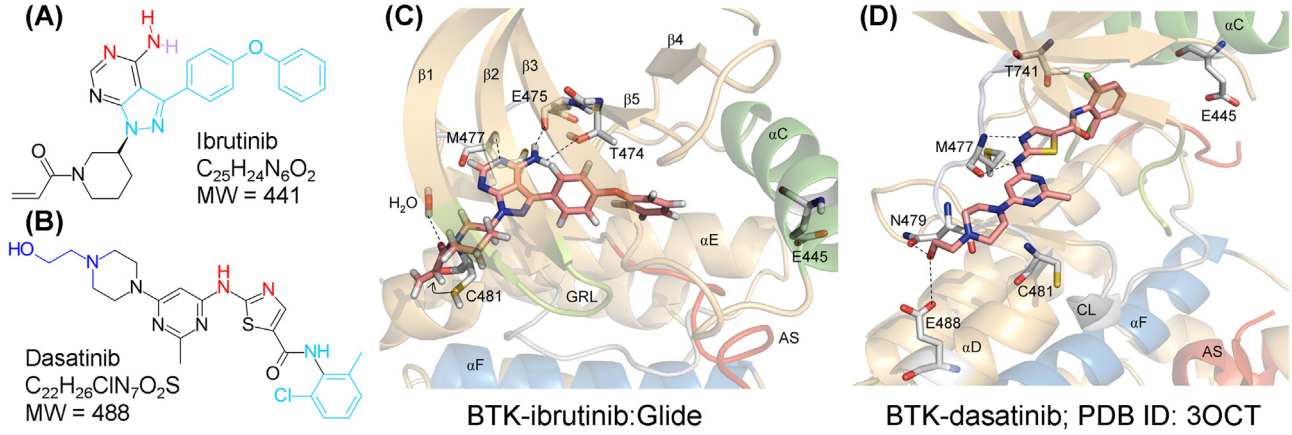

Fig. 7. (A) Ibrutinib. (B) Dasatinib. (C) Ibrutinib bound to BTK prepared with the Glide docking program [54]. (D) Dasatinib bound to BTK. The atoms of the drugs colored red interact with hinge residues; the lavender colored residue interacts with the T474 gatekeeper; the light blue residues occur within hydrophobic pockets and the dark blue residues interact with the solvent. AS, activation segment; CL, catalytic loop; GRL, Gly-rich loop.

or ofatumumab, or pembrolizumab, or ublituximab; (xiii) ibrutinib, CC-122, and obinutuzumab; (xiv) ibrutinib and BI 836826; (xv) ublituximab in combination with TGR-1202 with or without ibrutinib; (xvi) ibrutinib, venetoclax, and obinutuzumab; (xvii) a sequential regimen of bendamustine followed by ofatumumab and ibrutinib and then with ibrutinib and ofatumumab maintenance; and (xviii) ibrutinib and TGR-1202.

It might be advantageous to combine ibrutinib with idelalisib to block the activities of two members of the B cell receptor pathway (BTK and PLCγ2). Because these drugs are marketed by two different drug companies, this potential combined therapy is not being addressed. Owing to the cost of each of these medicines of more than $100,000 per year in the United States, such a combination would promise to lead to financial toxicity [28,52]. The mechanism of action of these drugs is listed in Table 3.

Of the more than 900 clinical trials focusing on mantle cell lymphoma, only 43 involve ibrutinib (www.clinicaltrials.gov). The latter trials include the following combinations of drugs: (i) ibrutinib and buparlisib; (ii) ibrutinib and palbociclib; (iii) ibrutinib vs. temsirolimus; (iv) ibrutinib and venetoclax; (v) ibrutinib, bendamustine, and rituximab; and (vi) ibrutinib, lenalidomide, and rituximab. Of the more than 400 Waldenström macroglobulinemia clinical trials, only 11 include ibrutinib. The following drug regimens are being explored for the treatment of this disorder: (i) ibrutinib and pembrolizumab; (ii) ibrutinib and rituximab; (iii) ibrutinib, rituximab, and bendamustine; and (iv) ibrutinib and pembrolizumab vs. idelalisib and pembrolizumab. Owing to the overexpression of the CDK4/6 activating cyclin D1 in most mantle cell lymphomas, the combination of ibrutinib with the CDK4/6 inhibitor palbociclib [28] represents a promising approach.

There are more than 1150 clinical trials exploring treatment options for diffuse large B cell lymphomas (DLBCLs), but only 25 of them consider ibrutinib. The following drug regimens are being tested for the treatment of this entity: (i) ibrutinib and rituximab, ifosfamide, carboplatin, and etoposide; (ii) ibrutinib and durvalumab; and (iii) ibrutinib and vistusertib. Of the more than 2100 clinical trials focusing on multiple myeloma, only 6 involve ibrutinib. The latter trials include the following combinations: (i) ibrutinib, dexamethasone, and pomalidomide or (ii) ibrutinib and carfilzomib with or without dexamethasone. Additionally, the following therapy is being studied for the treatment of acute myelogenous leukemia: ibrutinib, cytarabine, and idarubicin.

Besides hematological malignancies and lymphomas, ibrutinib combination therapy is being evaluated in several solid tumors. For example, ibrutinib with everolimus, paclitaxel, docetaxel, or cetuximab is being studied in the treatment of colorectal, gastric, renal cell, and urothelial carcinomas (www.clinicaltrials.gov). It is also under investigation as a monotherapy for the treatment of melanoma, carcinoid tumors of the gastrointestinal tract, and pancreatic neuroendocrine tumors. Moreover, it is being studied in combination with nab-paclitaxel and gemcitabine for the first line treatment of patients with metastatic pancreatic adenocarcinoma. Part of the rationale for the use of ibrutinib in these solid tumors involves the role of tumor-promoting inflammation in the pathogenesis of neoplastic diseases [53].

5. Binding of ibrutinib and dasatinib to BTK

No X-ray structural studies of ibrutinib (Fig. 7A) bound to BTK have been reported. To obtain an idea on the possible interaction of this drug with the enzyme, the Schrödinger Glide Suite (2016-1 release) was used to dock the drug into human BTK (with initially bound SureChEMBL14630168, PDB ID: 5FBN) [54]. The 4-amino group of the drug makes hydrogen bonds with the gatekeeper T474 and the first hinge residue E475 and the *N*3 group of the pyrazolo[3,4-*d*]pyrimidine core makes a hydrogen bond with the N—H group of M477 within the hinge (Fig. 7C). The drug makes hydrophobic contacts with L408 before the G-rich loop, V416 after the G-rich loop, A428 (CS7), M449 (RS3), V458 (Sh1), L460 within the αC-β4 loop, I472 before the hinge, Y476 within the hinge, N484 after the hinge, L528 (CS6), DFG-F540, and L542 within the activation segment. DFG-D539 makes van der Waals contact with the drug. The pose indicates that the thiol group of C481 is within 3 Å of the acrylamide group. Drugs such as ibrutinib [55] with an α,β-unsaturated carbonyl group undergo a Michael reaction, which involves the addition of a nucleophile (the −SH of cysteine) to the β-carbon of the unsaturated carbonyl congener to form a covalent Michael adduct.

Hydrogen bonding as seen in Fig. 7C along with hydrophobic interactions place the drug in a productive orientation within the ATP-binding pocket, which allows the covalent modification to proceed. Our classification of inhibitors based upon their interaction with protein kinases considers covalent modification as a Class VI inhibitor [30]. Prior to the modification, the drug binds noncovalently to an inactive enzyme with the DFG-Asp directed inward and with the αC-helix directed outward, thereby corresponding to a type I½A inhibitor as described in Section 7.

An X-ray structure of dasatinib (Fig. 7B) bound to BTK has been reported (PDB ID: 3OCT). The *N*3 of the thiazole group forms a hydrogen bond with the N—H group of M477 within the hinge while

Table 4
Classification of small molecule protein kinase inhibitors.[a]

Type	Subtype	Properties	FDA-approved drugs
I		Binds in the ATP-binding pocket of the active enzyme conformation	Alectinib, bosutinib, cabozantinib, ceritinib, crizotinib, dasatinib, erlotinib, gefitinib, lapatinib, palbociclib, pazopanib, ponatinib, ruxolitinib, tofacitinib, vandetanib
I½	A	Binds in the ATP-binding pocket of an inactive DFG-Asp in conformation extending to the back cleft	Dasatinib, lapatinib, lenvatinib, vemurafenib
	B	Same as I½A except that the drug does not extend into the back cleft	Erlotinib, sunitinib
II	A	Binds in the ATP-binding pocket of the inactive DFG-Asp out conformation extending to the back cleft	Axitinib, imatinib, nilotinib, regorafenib, sorafenib
	B	Same as IIA except that the drug does not extend into the back cleft	Bosutinib, crizotinib, nintedanib, sunitinib
III		Allosteric inhibitor that binds adjacent to the ATP site	Cobimetinib, trametinib
IV		Allosteric inhibitor that does not bind adjacent to the ATP site	Everolimus, sirolimus, temsirolimus
V		Bivalent inhibitor spanning two kinase regions	None
VI		Covalent inhibitor	Afatinib, ibrutinib, osimertinib

[a] Adapted from Ref. [30].

the amino group makes a hydrogen bond with the carbonyl group of the same residue. The oxygen of the terminal hydroxyethyl group forms hydrogen bonds with N479 within the hinge and with E488 within the αD helix (Fig. 7D). The drug makes hydrophobic contacts with L408 immediately before the G-rich loop, F413 within the G-rich loop, V416 after the loop, A428 (CS7), I429, M449 (RS3), V458 (Sh1), I472 before the hinge, Y476 within the hinge, L528 (CS6), and DFG-F540. Unlike ibrutinib, dasatinib fails to interact with L460, N484, and L542. Unlike dasatinib, ibrutinib fails to interact with F413 and I429. The DFG-Asp is in the inactive "out" conformation and the drug does not extend into the back pocket, criteria that make this antagonist a type IIB inhibitor [30].

6. Covalent protein kinase inhibitors

The United States Food and Drug Administration has approved three covalent protein kinase inhibitors for the treatment of various malignancies. Afatinib is approved as a first-line treatment for patients with NSCLC that possess exon 19 deletions or an exon 21 L858R mutation (www.brimr.org/PKI/PKIs.htm). It is also approved for the second-line treatment of patients with metastatic NSCLC that had progressed on platinum-based therapy. Osimertinib is approved as a second-line treatment for NSCLC patients with the *EGFR T790M* gatekeeper mutation, but who have become resistant to other EGFR protein kinase inhibitors such as such as erlotinib. As noted previously, ibrutinib is approved for the treatment of mantle cell lymphoma, chronic lymphoblastic leukemia, and Waldenström macroglobulinemia. As indicated by the interaction of ibrutinib with BTK (Fig. 7C), polar and hydrophobic interactions position the drug in an orientation that allows the covalent modification to proceed as the enzyme attacks the electrophilic portion of the drug to form a Michael adduct.

In a comprehensive analysis of the protein kinase cysteinome, Liu et al. mapped targetable cysteine residues in and around the ATP-binding pocket [56]. They described six distinct cysteine targets including a cysteine (i) within the Gly-rich loop that occurs in FGFR, (ii) in the roof of the pocket found in NEK2 and RSK enzymes, (iii) immediately preceding the DFG of VEGFR, ERK2, and GSK3β, (iv) in the solvent area found in JNKs, (v) in the catalytic loop of Kit and PDGFR, and (vi) after the hinge found in the EGFR family members ERBB1/2/4, the Src family member Blk, MKKa7, JAK3, and the TEC family including BMX, BTK, ITK, TEC, and TXK [55,56]. It is possible that some of the toxic effects and some of the therapeutic effects of ibrutinib are related to the modification of cysteine residues after the hinge in the last group of targets. Leproult et al. have also reported on the strategy and design of preparing selective covalent protein kinase inhibitors [57].

Covalent irreversible drugs had been disfavored as a drug class owing to safety and toxicity concerns [58]. However, aspirin is an irreversible inhibitor that has been in the medicinal armamentarium for more than a century. Roth et al. discovered that aspirin exerts its therapeutic effect by covalently modifying Ser530 of cyclooxygenase 1 by acetylation [59,60]. Rasagiline and selegiline, which are FDA approved for the treatment of Parkinson disease, are additional examples of irreversible enzyme inhibitors [61]. These acetylenic drugs, which are used as monotherapy in early Parkinson disease or as an adjunct therapy in more advanced cases, inhibit type B monoamine oxidase by forming a covalent adduct with the *N*5 of the monoamine oxidase FAD cofactor [62]. Moreover, covalent proton pump inhibitors that reduce stomach acid such as esomeprazole, lansoprazole, and omeprazole are effective, safe, and widely used in the treatment of dyspepsia, peptic ulcers, and gastroesophageal reflux [58]. These drugs form a cyclic sulfenamide that reacts with an essential proton pump cysteine to form an inactive disulfide adduct [63]. Moreover, the clinical success of ibrutinib, afatinib, and osimertinib has helped to overcome the bias against irreversible drug inhibitors.

7. Epilogue

The difference between active and inactive conformations is an important distinction when considering the regulation of protein kinase signaling. DFG-Asp in/out (active/inactive), αC-in/out (active/inactive), and the activation segment open/closed (active/inactive) represent the major conformational states. There are many subtleties in describing active and inactive conformations within this context. Sometimes the distinction of various DFG-Asp-in/out conformations may be difficult to discern by inspection, but we find that visualization of the location of RS2 of the R-spine (DFG-F) removes most of these ambiguities. A linear spine characterizes an active state while a non-linear or broken spine depicts an inactive state. Nevertheless, the classification of protein kinase structures and activity states in some instances is uncertain.

The interaction of each drug with a protein kinase target is unique. Nevertheless, it is useful to classify these interactions in order to apply them to the drug discovery process. We have classi-

fied these drugs into six possible types based upon the structures of the drug-enzyme complexes (Table 4) [30]. Type I drugs bind to the active conformation of the protein kinase with (i) the αC-helix directed inward, (ii) an open activation segment (iii) the DFG-Asp directed inward, and (iv) a linear R-spine. The type I½ drugs bind to an inactive enzyme conformation (closed activation segment or non-linear R-spine), but with the DGF-Asp directed inward as formulated by Zuccotto et al. [64]. We subdivided this class into type I½A drugs that extend into the back pocket while the type I½B drugs do not [30]. Preliminary data indicate that the type A drugs have an extended residence time while the type B drugs do not.

The type II drugs bind to the enzyme with the DFG-Asp directed outward, which corresponds to an inactive conformation [65]. The R-spine RS3, which occurs within the αC-helix, is displaced from RS2 and RS4. The IIA drugs occur in the front cleft, the gate area, and they extend into the back pocket while the type IIB drugs occur within the front cleft and gate area and do not extend into the back cleft [30]. Owing to the uniqueness of inactive protein kinase conformations when compared with the canonical active conformation, it was hypothesized that type II drugs would be more selective than type I drugs that bind to the prototypical active conformation. However, there is substantial overlap in the selectivity of type I and type II inhibitors so that the hypothesized advantages of targeting inactive conformations have not been realized [66]. The type III and IV inhibitors are allosteric in nature [67] and the type V drugs span two different protein kinase regions [68]. The type VI inhibitors including ibrutinib bind covalently with the enzyme [30]. Note that about half of the approved drugs bind to the active conformation of their target protein kinase and are type I inhibitors (Table 4).

That a given drug can bind to two different conformations of its protein kinase targets increases the complexity of inhibitor classification [30]. For example, bosutinib is a type I inhibitor of the Src protein-tyrosine kinase and a type IIB inhibitor of the Abl protein-tyrosine kinase. Sunitinib is a type I½B inhibitor of the protein-serine/threonine kinase CDK2 and a type IIB inhibitor of the Kit receptor protein-tyrosine kinase. Moreover, crizotinib is a type I inhibitor of the ALK receptor protein-tyrosine kinase and a type I½ B inhibitor of the c-Met receptor protein-tyrosine kinase. Adding to the complexity, erlotinib is a type I and I½B inhibitor of the epidermal growth factor receptor protein-tyrosine kinase. These findings suggest that protein kinase inhibitors lack conformational selectivity. Moreover, these results indicate that drugs occupying only the adenine pocket and gate area and excluding the back cleft may be interchangeable as type I, I½B, and IIB inhibitors. By inference, antagonists that also extend into the back cleft may function as type I½A and IIA inhibitors, but not type I inhibitors.

Targeting protein kinases for therapeutic purposes began earnestly in 2001 with the FDA approval of imatinib for the treatment of chronic myelogenous leukemia. The FDA has approved 32 small molecule protein kinase inhibitors for the treatment of various neoplastic and inflammatory disorders (www.brimr.org/PKI/PKIs.htm). All of these agents are orally effective except for temsirolimus, which is given by intravenous infusion for the treatment of advanced renal cell carcinoma. Of the more than 500 human protein kinases, only three dozen protein kinases are currently being targeted for the treatment of a variety of illnesses. The FDA is approving small molecule protein kinase inhibitors at a rate of about three per year and there is no indication that this rate of approval will abate. Nearly all of the current therapeutic indications are for neoplastic disorders including carcinomas, leukemias, and lymphomas. The approvals of (i) the Janus protein-tyrosine kinase family inhibitor tofacitinib for the treatment of rheumatoid arthritis in 2012 and (ii) the fibroblast growth factor, platelet-derived growth factor, and vascular endothelial growth factor receptor protein-tyrosine kinase inhibitor nintedanib for the treatment of idiopathic pulmonary fibrosis in 2014 represent an expanded therapeutic range that one anticipates will increase in the future.

Conflict of interest

The author is unaware of any affiliations, memberships, or financial holdings that might be perceived as affecting the objectivity of this review.

Acknowledgement

The author thanks Laura M. Roskoski for providing editorial and bibliographic assistance.

References

[1] D. Vetrie, I. Vorechovský, P. Sideras, J. Holland, A. Davies, F. Flinter, et al., The gene involved in X-linked agammaglobulinaemia is a member of the src family of protein-tyrosine kinases, Nature 361 (1993) 226–233, Erratum in: Nature 1993;364:362.
[2] S. Tsukada, D.C. Saffran, D.J. Rawlings, O. Parolini, R.C. Allen, L. Cohen, et al., Deficient expression of a B cell cytoplasmic tyrosine kinase in human X-linked agammaglobulinemia, Cell 72 (1993) 279–290.
[3] J.D. Thomas, P. Sideras, C.I. Smith, I. Vorechovský, V. Chapman, W.E. Paul, Colocalization of X-linked agammaglobulinemia and X-linked immunodeficiency genes, Science 261 (1993) 355–358.
[4] D.J. Rawlings, D.C. Saffran, S. Tsukada, D.A. Largaespada, J.C. Grimaldi, L. Cohen, et al., Mutation of unique region of Bruton's tyrosine kinase in immunodeficient XID mice, Science 261 (1993) 358–361.
[5] O.C. Bruton, A decade with agammaglobulinemia, J. Pediatr. 60 (1962) 672–676.
[6] A. Wiestner, The role of B-cell receptor inhibitors in the treatment of patients with chronic lymphocytic leukemia, Haematologica 100 (2015) 1495–1507.
[7] A. Mócsai, J. Ruland, V.L. Tybulewicz, The SYK tyrosine kinase: a crucial player in diverse biological functions, Nat. Rev. Immunol. 10 (2010) 387–402.
[8] R.W. Hendriks, S. Yuvaraj, L.P. Kil, Targeting Bruton's tyrosine kinase in B cell malignancies, Nat. Rev. Cancer 14 (2014) 219–232.
[9] R. Roskoski Jr., RAF protein-serine/threonine kinases: structure and regulation, Biochem. Biophys. Res. Commun. 399 (2010) 313–317.
[10] R. Roskoski Jr., MEK1/2 dual-specificity protein kinases: structure and regulation, Biochem. Biophys. Res. Commun. 417 (2012) 5–10.
[11] R. Roskoski Jr., ERK1/2 MAP kinases: structure, function, and regulation, Pharmacol. Res. 66 (2012) 105–143.
[12] R. Roskoski Jr., A historical overview of protein kinases and their targeted small molecule inhibitors, Pharmacol. Res. 100 (2015) 1–23.
[13] M. Spaargaren, E.A. Beuling, M.L. Rurup, H.P. Meijer, M.D. Klok, S. Middendorp, et al., The B cell antigen receptor controls integrin activity through Btk and PLCγ2, J. Exp. Med. 198 (2003) 1539–1550.
[14] G. Manning, D.B. Whyte, R. Martinez, T. Hunter, S. Sudarsanam, The protein kinase complement of the human genome, Science 298 (2002) 1912–1934.
[15] R. Roskoski Jr., Src protein-tyrosine kinase structure and regulation, Biochem. Biophys. Res. Commun. 324 (2004) 1155–1164.
[16] R. Roskoski Jr., Src protein-tyrosine kinase structure, mechanism, and small molecule inhibitors, Pharmacol. Res. 94 (2015) 9–25.
[17] T. Kawakami, W. Xiao, Phospholipase C-β in immune cells, Adv. Biol. Regul. 53 (2013) 249–257.
[18] S.K. Hanks, T. Hunter, Protein kinases 6. The eukaryotic protein kinase superfamily: kinase (catalytic) domain structure and classification, FASEB J. 9 (1995) 576–596.
[19] D.R. Knighton, J.H. Zheng, L.F. Ten Eyck, V.A. Ashford, N.H. Xuong, S.S. Taylor, et al., Crystal structure of the catalytic subunit of cyclic adenosine monophosphate-dependent protein kinase, Science 253 (1991) 407–414.
[20] D.R. Knighton, J.H. Zheng, L.F. Ten Eyck, N.H. Xuong, S.S. Taylor, J.M. Sowadski, Structure of a peptide inhibitor bound to the catalytic subunit of cyclic adenosine monophosphate-dependent protein kinase, Science 253 (1991) 414–420.
[21] S.S. Taylor, A.P. Kornev, Protein kinases: evolution of dynamic regulatory proteins, Trends Biochem. Sci. 36 (2011) 65–77.
[22] S.S. Taylor, M.M. Keshwani, J.M. Steichen, A.P. Kornev, Evolution of the eukaryotic protein kinases as dynamic molecular switches, Philos. Trans. R Soc. Lond. B: Biol. Sci. 367 (2012) 2517–2528.
[23] B. Nolen, S. Taylor, G. Ghosh, Regulation of protein kinases; controlling activity through activation segment conformation, Mol. Cell 15 (2004) 661–675.
[24] D.J. Rawlings, A.M. Scharenberg, H. Park, M.I. Wahl, S. Lin, R.M. Kato, et al., Activation of BTK by a phosphorylation mechanism initiated by SRC family kinases, Science 271 (1996) 822–825.
[25] A.P. Kornev, N.M. Haste, S.S. Taylor, L.F. Ten Eyck, Surface comparison of active and inactive protein kinases identifies a conserved activation mechanism, Proc. Natl. Acad. Sci. U. S. A. 103 (2006) 17783–17788.
[26] A.P. Kornev, S.S. Taylor, L.F. Ten Eyck, A helix scaffold for the assembly of active protein kinases, Proc. Natl. Acad. Sci. U. S. A. 105 (2008) 14377–14382.

[27] R. Roskoski Jr., Janus kinase (JAK) inhibitors in the treatment of inflammatory and neoplastic diseases, Pharmacol. Res. 111 (2016) 784–803.
[28] R. Roskoski Jr., Cyclin-dependent protein kinase inhibitors including palbociclib as anticancer drugs, Pharmacol. Res. 111 (2016) 784–803.
[29] H.S. Meharena, P. Chang, M.M. Keshwani, K. Oruganty, A.K. Nene, N. Kannan, et al., Deciphering the structural basis of eukaryotic protein kinase regulation, PLoS Biol. 11 (2013) e1001680.
[30] R. Roskoski Jr., Classification of small molecule protein kinase inhibitors based upon the structures of their drug-enzyme complexes, Pharmacol. Res. 103 (2016) 26–48.
[31] O.P. van Linden, A.J. Kooistra, R. Leurs, I.J. de Esch, C. de Graaf, KLIFS: a knowledge-based structural database to navigate kinase-ligand interaction space, J. Med. Chem. 57 (2014) 249–277.
[32] Q. Wang, E.M. Vogan, L.M. Nocka, C.E. Rosen, J.A. Zorn, S.C. Harrison, et al., Autoinhibition of Bruton's tyrosine kinase (Btk) and activation by soluble inositol hexakisphosphate, Elife (2015) 4, http://dx.doi.org/10.7554/eLife.06074.
[33] H.C. Kluin-Nelemans, E. Hoster, O. Hermine, J. Walewski, M. Trneny, C.H. Geisler, et al., Treatment of older patients with mantle-cell lymphoma, N. Engl. J. Med. 367 (2012) 520–531.
[34] A.A. Inamdar, A. Goy, N.M. Ayoub, C. Attia, L. Oton, V. Taruvai, et al., Mantle cell lymphoma in the era of precision medicine-diagnosis, biomarkers and therapeutic agents, Oncotarget (2016), http://dx.doi.org/10.18632/oncotarget.8961, Epub ahead of print.
[35] M.L. Wang, S. Rule, P. Martin, A. Goy, R. Auer, B.S. Kahl, et al., Targeting BTK with ibrutinib in relapsed or refractory mantle-cell lymphoma, N. Engl. J. Med. 369 (2013) 507–516.
[36] R.A. de Claro, K.M. McGinn, N. Verdun, S.L. Lee, H.J. Chiu, H. Saber, et al., FDA approval: ibrutinib for patients with previously treated mantle cell lymphoma and previously treated chronic lymphocytic leukemia, Clin. Cancer Res. 21 (2015) 3586–3590.
[37] G. Fabbri, R. Dalla-Favera, The molecular pathogenesis of chronic lymphocytic leukaemia, Nat. Rev. Cancer 16 (2016) 145–162.
[38] M. Hallek, B.D. Cheson, D. Catovsky, F. Caligaris-Cappio, G. Dighiero, H. Döhner, et al., Guidelines for the diagnosis and treatment of chronic lymphocytic leukemia: a report from the International Workshop on Chronic Lymphocytic Leukemia updating the National Cancer Institute-Working Group 1996 guidelines, Blood 111 (2008) 5446–5456, Erratum in: Blood 2008;112:5259.
[39] C.M. Vela, A. McBride, S.M. Jaglowski, L.A. Andritsos, Ibrutinib for treatment of chronic lymphocytic leukemia, Am. J. Health. Syst. Pharm. 73 (2016) 367–375.
[40] J.C. Byrd, R.R. Furman, S.E. Coutre, I.W. Flinn, J.A. Burger, K.A. Blum, et al., Targeting BTK with ibrutinib in relapsed chronic lymphocytic leukemia, N. Engl. J. Med. 369 (2013) 32–42.
[41] J.C. Byrd, R.R. Furman, S.E. Coutre, J.A. Burger, K.A. Blum, M. Coleman, et al., Three-year follow-up of treatment-naïve and previously treated patients with CLL and SLL receiving single-agent ibrutinib, Blood 125 (2015) 2497–2506.
[42] J.A. Woyach, R.R. Furman, T.M. Liu, H.G. Ozer, M. Zapatka, A.S. Ruppert, et al., Resistance mechanisms for the Bruton's tyrosine kinase inhibitor ibrutinib, N. Engl. J. Med. 370 (2014) 2286–2294.
[43] K.J. Maddocks, A.S. Ruppert, G. Lozanski, N.A. Heerema, W. Zhao, L. Abruzzo, et al., Etiology of ibrutinib therapy discontinuation and outcomes in patients with chronic lymphocytic leukemia, JAMA Oncol. 1 (2015) 80–87.
[44] A.R. Johnson, P.B. Kohli, A. Katewa, E. Gogol, L.D. Belmont, R. Choy, et al., Battling Btk mutants with noncovalent inhibitors that overcome cys481 and thr474 mutations, ACS Chem. Biol. (2016), Epub ahead of print.
[45] M. Azam, M.A. Seeliger, N.S. Gray, J. Kuriyan, G.Q. Daley, Activation of tyrosine kinases by mutation of the gatekeeper threonine, Nat. Struct. Mol. Biol. 15 (2008) 1109–1118.
[46] S. Cheng, A. Guo, P. Lu, J. Ma, M. Coleman, Y.L. Wang, Functional characterization of BTK(C481S) mutation that confers ibrutinib resistance: exploration of alternative kinase inhibitors, Leukemia 29 (2015) 895–900.
[47] O. Hantschel, U. Rix, U. Schmidt, T. Bürckstümmer, M. Kneidinger, G. Schütze, et al., The Btk tyrosine kinase is a major target of the Bcr-Abl inhibitor dasatinib, Proc. Natl. Acad. Sci. U. S. A. 104 (2007) 13283–13288.
[48] M.A. Gertz, Waldenström macroglobulinemia: 2015 update on diagnosis, risk stratification, and management, Am. J. Hematol. 90 (2015) 346–354.
[49] S.P. Treon, C.K. Tripsas, K. Meid, D. Warren, G. Varma, R. Green, et al., Ibrutinib in previously treated Waldenström's macroglobulinemia, N. Engl. J. Med. 372 (2015) 1430–1440.
[50] A. Oza, S.V. Rajkumar, Waldenstrom macroglobulinemia: prognosis and management, Blood Cancer J. 5 (2015) e394.
[51] S.P. Treon, How I treat Waldenström macroglobulinemia, Blood 126 (2015) 721–732.
[52] S.Y. Zafar, J.M. Peppercorn, D. Schrag, D.H. Taylor, A.M. Goetzinger, X. Zhong, et al., The financial toxicity of cancer treatment: a pilot study assessing out-of-pocket expenses and the insured cancer patient's experience, Oncologist 18 (2013) 381–390.
[53] D. Hanahan, R.A. Weinberg, Hallmarks of cancer: the next generation, Cell 144 (2011) 646–674.
[54] R.A. Friesner, J.L. Banks, R.B. Murphy, T.A. Halgren, J.J. Klicic, D.T. Mainz, et al., Glide: a new approach for rapid, accurate docking and scoring: 1. Method and assessment of docking accuracy, J. Med. Chem. 47 (2004) 1739–1749.
[55] Z. Pan, H. Scheerens, S.J. Li, B.E. Schultz, P.A. Sprengeler, L.C. Burrill, et al., Discovery of selective irreversible inhibitors for Bruton's tyrosine kinase, ChemMedChem 2 (2007) 58–61.
[56] Q. Liu, Y. Sabnis, Z. Zhao, T. Zhang, S.J. Buhrlage, L.H. Jones, et al., Developing irreversible inhibitors of the protein kinase cysteinome, Chem. Biol. 20 (2013) 146–159.
[57] E. Leproult, S. Barluenga, D. Moras, J.M. Wurtz, N. Winssinger, Cysteine mapping in conformationally distinct kinase nucleotide binding sites: application to the design of selective covalent inhibitors, J. Med. Chem. 54 (2011) 1347–1355.
[58] J. Singh, R.C. Petter, T.A. Baillie, A. Whitty, The resurgence of covalent drugs, Nat. Rev. Drug Discov. 10 (2011) 307–317.
[59] G.J. Roth, N. Stanford, P.W. Majerus, Acetylation of prostaglandin synthase by aspirin, Proc. Natl. Acad. Sci. U. S. A. 72 (1975) 3073–3076.
[60] R.M. Botting, Vane's discovery of the mechanism of action of aspirin changed our understanding of its clinical pharmacology, Pharmacol. Rep. 62 (2010) 518–525.
[61] A.H. Schapira, Monoamine oxidase B inhibitors for the treatment of Parkinson's disease: a review of symptomatic and potential disease-modifying effects, CNS Drugs 25 (2011) 1061–1071.
[62] A.L. Maycock, R.H. Abeles, J.I. Salach, T.P. Singer, The structure of the covalent adduct formed by the interaction of 3-dimethylamino-1-propyne and the flavine of mitochondrial amine oxidase, Biochemistry 15 (1976) 114–125.
[63] R.M. Ward, G.L. Kearns, Proton pump inhibitors in pediatrics: mechanism of action, pharmacokinetics, pharmacogenetics, and pharmacodynamics, Paediatr. Drugs 15 (2013) 119–131.
[64] F. Zuccotto, E. Ardini, E. Casale, M. Angiolini, Through the gatekeeper door: exploiting the active kinase conformation, J. Med. Chem. 53 (2010) 2681–2694.
[65] A.C. Dar, K.M. Shokat, The evolution of protein kinase inhibitors from antagonists to agonists of cellular signaling, Annu. Rev. Biochem. 80 (2011) 769–795.
[66] Z. Zhao, H. Wu, L. Wang, Y. Liu, S. Knapp, Q. Liu, N.S. Gray, Exploration of type II binding mode: a privileged approach for kinase inhibitor focused drug discovery? ACS Chem. Biol. 9 (2014) 1230–1241.
[67] L.K. Gavrin, E. Saiah, Approaches to discover non-ATP site inhibitors, Med. Chem. Commun. 4 (2013) 41.
[68] V. Lamba, I. Ghosh, New directions in targeting protein kinases: focusing upon true allosteric and bivalent inhibitors, Curr. Pharm. Des. 18 (2012) 2936–2945.